RESEARCH ARTICLE

Insights into yeast adaptive response to the agricultural fungicide mancozeb: A toxicoproteomics approach

Pedro M. Santos, Tânia Simões and Isabel Sá-Correia

IBB – Institute for Biotechnology and Bioengineering, Centre for Biological and Chemical Engineering, Instituto Superior Técnico, Lisboa, Portugal

Received: May 24, 2008
Revised: August 3, 2008
Accepted: September 5, 2008

Toxicogenomics has the potential to elucidate gene–environment interactions to identify genes that are affected by a particular chemical at the early stages of the toxicological response and to establish parallelisms between different organisms. The fungicide mancozeb, widely used in agriculture, is an ethylene-bis-dithiocarbamate complex with manganese and zinc. Exposure to this pesticide has been linked to the development of idiopathic Parkinson's disease and cancer. Given that many signalling pathways and their molecular components are substantially conserved among eukaryotic organisms, we used *Saccharomyces cerevisiae* to get insights into the molecular mechanisms of mancozeb toxicity and adaptation based on expression proteomics. The early global response to mancozeb was analysed by quantitative proteomics using 2-DE. The target genes (*e.g. TSA1*, *TSA2*, *SOD1*, *SOD2*, *AHP1*, *GRE2*, *GRX1*, *CYS3*, *PRE3*, *PRE6*, *PRE8*, *PRE9*, *EFT1*, *RPS5*, *TIF11*, *HSP31*, *HSP26*, *HSP104*, *HSP60*, *HSP70*-family) and the putative main transcription activators (*e.g.* Yap1, Msn2/Msn4, Met4, Hsf1, Aft1, Pdr1, Skn7, Rpn4p, Gcn4) of the complex mancozeb-induced expression changes are related with yeast response to stress, in particular to oxidative stress, protein translation initiation and protein folding, disassembling of protein aggregates and degradation of damaged proteins. Our results also suggest that this study provided powerful indications that may be useful to expand the knowledge obtained in yeast not only to the global response to mancozeb toxicity in phytopathogenic fungi but also to humans.

Keywords:
Dithiocarbamates / Mancozeb / *Saccharomyces cerevisiae* / Stress response / Toxicogenomics

1 Introduction

Chronic exposure to several pesticides has been linked to the development of Parkinsonism symptoms in mammals whose etiology involves both genetic and environmental components [1–4]. Elevated risks associated with several pesticides, including maneb (MB) and mancozeb (MZ), were reinforced by recent data obtained from self-reports of Parkinson's disease (PD) from licensed private pesticide applicators participating in the Agricultural Health Study carried out in USA [5]. MZ is a mixture of manganese- (MB) and zinc- (zineb) ethylene-bis-dithiocarbamates (EBDC) (Mn/Zn, 9:1). MZ and other metal–EBDC fungicides also lead to other chronic adverse health effects such as structural and functional alterations of gonads [6] and thyroid [7]. MZ and MB are equipotent neurotoxicants and a recent study on the mechanisms of neural damage associated with MZ exposure has determined the role that ROS, generated by Mn-containing EBDC fungicides, play in toxicity [8]. Fungicide exposure was associated with mitochondrial uncoupling and inhibition of mitochondrial

Correspondence: Professor Isabel Sá-Correia, IBB, Institute for Biotechnology and Bioengineering, Centre for Biological and Chemical Engineering, Instituto Superior Técnico, Av. Rovisco Pais, 1049-001, Lisboa, Portugal
E-mail: isacorreia@ist.utl.pt
Fax: +351-218419199

Abbreviations: Cys3p, cystathionine γ-lyase; **EBDC,** ethylene-bis-dithiocarbamate; **FMN,** flavin mononucleotide; **GSH,** glutathione; **MB,** maneb; **MZ,** mancozeb; **PD,** Parkinson's disease; **SOD,** superoxide dismutase

respiration is known to increase free radical production [8]. DNA damage and apoptosis induction by MZ in rat cells is also related to an oxidative mechanism [9]. Despite its toxicity, MZ is one of the most widely used agricultural fungicides [10] and has maintained its efficacy against a broad spectrum of phytopathogenic fungi. The exact mode of action is not known but it has been proposed to act by inhibiting enzyme activity as its high reactivity was related to metal-chelating ability and high affinity for –SH group containing proteins [11, 12].

The new interdisciplinary area of environmental toxicogenomics offers a tool to directly monitor the earliest stages of the toxicological response [13]. Such alterations of global gene expression that can be monitored by microarrays and expression proteomics, occur almost immediately following exposure to the toxicant whereas the clinical manifestation of toxicity might take days or even years to develop. Since, there is increasing evidence that chemicals with similar toxicological properties produce a characteristic gene expression signature profile [14], the assessment of changes occurring at the level of gene expression may potentially provide earlier and more sensitive biomarker(s) of a toxic response than traditional toxicological methods. To gain more insights into the global mechanisms underlying MZ toxicity and the cell response to this fungicide, we examined the variations occurring in protein expression level during the period of adaptation of a cell population of *Saccharomyces cerevisiae* to a moderate concentration of MZ using a proteomic approach based on 2-DE. The yeast *S. cerevisiae* is a very useful eukaryotic experimental model for environmental toxicogenomic studies [13]. Given that many signalling pathways and their molecular components are substantially conserved among eukaryotic organisms, model systems, in particular yeast, are being successfully used to examine the effects of environmental toxicants on the expression and function of these fundamental pathways in less genetically accessible eukaryotes [13]. The *FLR1* gene encoding a multidrug resistance transporter member of the 12-spanner H^+-drug antiporter family was recently identified as determinant of resistance to MZ in yeast [15]. The dramatic transcriptional activation of *FLR1* was registered following sudden yeast exposure to MZ as this activation was fully dependent on the presence of the b-ZIP transcription factor, Yap1p, and reduced (by 50%) in the absence of Rpn4p, Yrr1p or Pdr3p transcription factors [15].

The data obtained in the present study provided an additional number of new mechanistic clues into the underlying global response to MZ toxicity in yeast. Specifically, they highlighted the importance of the yeast response to stress, in particular the induction of a battery of oxidant defence genes and heat shock genes encoding chaperone proteins required for protein folding and recovery, and genes involved in the degradation of damaged proteins and of the inhibition of protein translation.

2 Materials and methods

2.1 Strains and media

S. cerevisiae BY4741 (*MAT***a**, *his3Δ1, leu2Δ0, met15Δ0, ura3Δ0*) was obtained from the Euroscarf collection (http://web.uni-frankfurt.de/fb15/mikro/euroscarf/index.html). Cells were batch-cultured at 30°C, with orbital agitation (250 rpm). The minimal growth medium MM4 used for cultivation of BY4741 contained (*per* litre): 1.7 g yeast nitrogen base without amino acids or NH_4^+ (Difco), 20 g glucose (Merck), 2.65 g $(NH_4)_2SO_4$ (Merck), 20 mg methionine (Merck), 20 mg histidine (Merck), 60 mg leucine (Sigma) and 20 mg uracil (Sigma). This basal medium, at pH 4.5, was either or not supplemented with 2 mg/L of the fungicide MZ (Riedel-de Haën). Growth curves were followed by measuring culture OD at 600 nm ($OD_{600\,nm}$). Inocula were obtained by cultivation of yeast cells in the absence of fungicide until mid-exponential phase, at a standardized $OD_{600\,nm} = 0.6 \pm 0.01$, and used to prepare main cultures with an initial $OD_{600\,nm} = 0.2 \pm 0.01$.

2.2 Sampling and protein extraction for 2-DE

The BY4741 proteomes were compared based on Sample A and B. Sample A, corresponded to a yeast population grown in MM4 medium and harvested during exponential growth at the standardized culture $OD_{600\,nm}$, 0.6. Sample B, corresponded to Sample A cell population inoculated in MM4 medium supplemented with 2 mg/L of MZ (initial $OD_{600\,nm}$, 0.2 ± 0.01) and incubated for 5 h in this medium. Sample B was thus harvested in the middle of fungicide-induced growth latency. The incubation of the same Sample A for 5 h in unsupplemented medium lead to an exponential yeast cell population that exhibit a physiological state identical to sample A cells. The two different culture samples, A and B, were harvested by centrifugation, washed with cold distilled water and the pellets immediately stored at −80°C until used. Each soluble protein extract was obtained from cell pellets resulting from three independent culture samples. Briefly, after thawed in ice, three cell pellets (corresponding to the same experimental condition) were pooled together, by resuspension in 0.9% NaCl followed by centrifugation, and resuspended in 2 mL of lysis buffer with the following composition: tris base 10 mM, pH 11 and protease inhibitors (10 mg/mL leupeptine; 1 mg/mL pepstatine A; 20 mg/mL aprotinine; 2 mg/mL trypsin/quimotrypsin inhibitor; 1.5 mg/mL benzamidine; 1 mM PMSF, all obtained from Sigma), and cell lysis was accomplished by consecutive steps of vortexing and cooling in the presence of an equal volume of glass beads (ϕ = 425–600 μm; Sigma). After addition of 2 mL lysis buffer, the mixture was centrifugated at $1000 \times g$, 40°C, during 5 min to separate cell debris and glass beads from the supernatant, designated supernatant I. Cell pellets were disrupted again as described above. The resulting supernatant, designated supernatant II, was mixed with

supernatant I, and the mixture was clarified by centrifugation at 3000 × *g*, 4°C, during 10 min. The soluble protein fraction was obtained by ultracentrifugation of this clarified supernatant at 100 000 × *g* during 90 min at 4°C. The protein concentration of these extracts was quantified using the BCA protein assay kit (Novagen). Total protein (700 μg) was then precipitated using 2D-CleanUp kit (GE Healthcare) and pellets resuspended in 450 μL of rehydration solution (9 M urea, 2% w/v CHAPS, 0.5% w/v Pharmalytes 3–10, 15 mM DTT and traces of bromophenol blue). The mixture was homogenized and left to stand at room temperature for 3 h. These protein samples were then centrifuged (10 000 × *g* for 5 min) and the supernatant transferred to clean 1.5 mL microcentrifuge tubes.

2.3 2-DE

2-DE was performed according to Santos *et al*. [16]. The protein samples were pipetted from 1.5 mL microcentrifuge tubes into the strip holders (Amersham Biosciences) and dry 24 cm IPG strips (Immobiline DryStrips pH 3–10; GE Healthcare) were positioned in the strip holders with the gel side down, avoiding entrapment of bubbles underneath the strip. The strips were then covered with 3 mL of DryStrip Cover Fluid (GE Healthcare) and the strip holders lidded. Strip rehydration was performed for 4 h at 0 V followed by 14 h at 30 V as the first step of the Ettan IPGphor focusing unit (GE Healthcare) protocol. IEF was carried out as described before [16]. After IEF, strips were immediately used for the second dimension separation. Briefly, strips were incubated in equilibration buffer (2% w/v SDS, 50 mM Tris-HCl pH 8.8, 6 M urea, 30% v/v glycerol and traces of bromophenol blue) containing 10 mg/mL DTT followed by incubation in the same buffer containing 25 mg/mL iodoacetamide. Strips were applied into 1.5 mm thick 12% w/v SDS-polyacrylamide gels. Proteins were separated at 2.5 W/gel for 30 min and 17 W/gel for 5 h.

2.4 Protein detection

Protein spots were detected by Coomassie staining. After the second dimension run, gel cassettes were opened and the gels carefully removed and placed in fixing solution (10% v/v acetic acid, 30% v/v ethanol) for 1 h. Gels were then stained using hot Coomassie solution (0.5% w/v CBB R-350 in 10% v/v acetic acid) overnight. Then, gels were washed with 10% v/v acetic acid solution during 24 h. At least 2 h prior to drying, gels were placed in 500 mL of dehydrating solution (35% v/v ethanol, 2% v/v glycerol). Afterwards, gels were placed between two sheets of porous cellophane wetted in dehydration solution, and locked into the Hoefer Easy Breeze drying frames (GE Healthcare). Gels were then left to dry at room temperature for at least 48 h.

2.5 Analysis of protein expression levels

In total, six 2-DE gels of each experimental condition (control and MZ treatment), corresponding to triplicates of two biological samples *per* condition, were analysed. The triplicates were performed to reduce technical variations that may occur across different separations. Each biological sample (*per* condition) was prepared by pooling together cell samples obtained from three independent growth experiments to reduce biological variation (as indicated in Section 2.2).

After drying, gels were scanned (Umax UTA III image Scanner; GE Healthcare) and the corresponding gel images were analysed using Progenesis SameSpots (Nonlinear Dynamics). Protein spots were identified by using the automatic spot detection algorithm. Individual spot volumes were normalized against total spot volumes for a given gel. Averages for each growth condition were then compared by their normalized volume using one-way ANOVA between-group test. Only statistically significant spots ($p<0.05$) were selected for analysis. In a few cases (indicated in the results section) spots with p between 0.05 and 0.1 were also analysed. Differential expression between different experimental conditions was quantified and a threshold of at least a 1.5-fold increase or 0.7-fold decrease between averaged gels was considered. Spots that showed evidence of saturation were not included for further analysis.

2.6 Identification of proteins

Identification of spots of possible interest was performed by PMF in the proteomics unit at the Centro Nacional de Investigaciones Cardiovasculares Carlos III, Madrid, Spain (CNIC Foundation), as a paid service. Protein spots were excised manually from polyacrylamide gels and then digested automatically using a Proteineer DP protein digestion station (Bruker-Daltonics, Bremen, Germany). The digestion protocol used was that of Shevchenko *et al.* [17] with minor variations; gel plugs were submitted to reduction with 10 mM DTT (GE Healthcare) in 50 mM ammonium bicarbonate (99.5% purity; Sigma Chemical, St. Louis, MO, USA) and alkylation with 55 mM iodoacetamide (Sigma Chemical) in 50 mM ammonium bicarbonate. The gel pieces were then rinsed with 50 mM ammonium bicarbonate and ACN (Gradient Grade; Merck, Darmstadt, Germany) and dried under a stream of nitrogen. Modified porcine trypsin (Sequencing Grade; Promega, Madison, WI, USA) at a final concentration of 13 ng/μL in 50 mM ammonium bicarbonate was added to the dry gel pieces and the digestion proceeded at 37°C for 6 h. Finally, 0.5% v/v TFA (99.5% purity; Sigma Chemical) was added for peptide extraction. An aliquot of the above digestion solution was mixed with an aliquot of CHCA (Bruker-Daltonics) in 33% v/v aqueous ACN and 0.1% v/v TFA. This mixture was deposited onto a 600 μm AnchorChip MALDI probe (Bruker-Daltonics) and allowed to dry at room temperature. MALDI-MS(/MS) data were obtained using an Ultraflex TOF mass spectrometer (Bruker-Daltonics) equip-

ped with a LIFT-MS/MS device [18]. Spectra were acquired in the positive-ion mode at 50 Hz laser frequency, and 100–1500 individual spectra were averaged. For fragment-ion analysis in the tandem TOF/TOF mode, precursors were accelerated to 8 kV and selected in a timed-ion gate. Fragment ions generated by laser-induced decomposition of the precursor were further accelerated by 19 kV in the LIFT cell and their masses were analysed after passing the ion reflector. Measurements were in part performed using post-LIFT metastable suppression, which allowed removal of precursor and metastable-ion signals produced after extraction out of the second-ion source. Detailed analysis of peptide mass mapping data was performed using flexAnalysis software (Bruker-Daltonics). Internal calibration of MALDI-TOF mass spectra was performed using two trypsin autolysis ions with $m/z = 842.510$ and $m/z = 2211.105$; for MALDI-MS/MS, calibrations were performed with fragment-ion spectra obtained for the proton adducts of a peptide mixture covering the 800–3200 m/z region. MALDI-MS and MS/MS data were combined through MS BioTools program (Bruker-Daltonics) to search the NCBInr database using MASCOT software (Matrix Science, London, UK) [19].

3 Results and discussion

3.1 Alteration of yeast growth curve and proteome in response to mancozeb

When a cell population of *S. cerevisiae* BY4741, in the exponential phase of growth in the absence of MZ, was introduced into the same basal growth medium supplemented with 2 mg/L of MZ, no significant increase of culture $OD_{600\,nm}$ was observed for a period of about 10 h (Fig. 1). During this MZ-induced growth latency, cell viability declined (results not shown). The growth curve registered in MZ-supplemented medium contrasts with the growth curve registered in unsupplemented medium where exponential growth was immediately resumed. When, after a period of growth latency, the viable population resumed cell division under MZ stress, the specific growth rate during exponential growth was lower than the specific growth rate registered in unsupplemented medium (Fig. 1).

After 5 h of inoculation in MZ-supplemented growth medium, the unadapted yeast population was in the middle of the period of duration of MZ-induced latency and the level of expression of the multidrug resistance transporter Flr1p was maximal [15]. After the same 5 h of incubation in the absence of the fungicide, the yeast population was in the exponential phase of growth, in the same physiological state as the cells used as inoculum (control cells). The proteomes of these two samples, A and B (described in Section 2) were separated by 2-DE and about 1600 protein spots were consistently separated in each gel within a p*I* range from pH 3 to pH 10 and a molecular mass ranging from 12 to 140 kDa. To identify the up- or downregulated proteins in response to MZ stress, a 2-DE reference map was prepared using the proteins present in MZ-stressed cells sample B (Fig. 2).

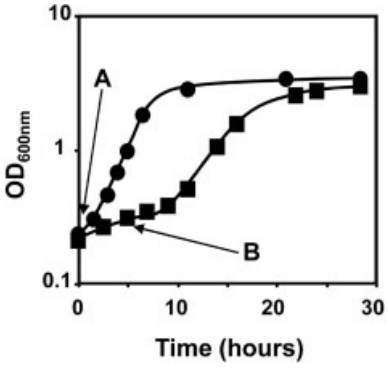

Figure 1. Growth curves of *S. cerevisiae* BY4741 in MM4 medium (●) or in this medium supplemented with 2 mg/L mancozeb (■). Cells used as inoculum were grown in the absence of fungicide and harvested in the exponential growth phase. Growth was followed by measuring culture $OD_{600\,nm}$. The growth curves presented are representative of at least three independent growth experiments. The arrows indicate the times of cultivation at which samples for 2-D PAGE were harvested.

Although this expression proteomic analysis, based on the preliminary comparison of the proteomes of MZ-stressed and-unstressed-yeast cells, could not assess the alterations registered in all the genome expressed genes, as virtually possible by transcriptomic analysis based on DNA microarrays, it offered a chance to identify the alterations occurring in 260 positively identified protein spots, corresponding to 145 different proteins (Table A of Supporting Information). For a subgroup of these 145 different proteins, more than one protein form was present in the 2-DE map (Table B of the Supporting Information). The proteins whose relative abundance was considered to vary in response to MZ (equal or above 1.5-fold and equal or below 0.7-fold for the upregulated or the downregulated proteins, respectively) (Table 1), were clustered into functional groups, according to SGD (http://www.yeastgenome.org/) and CYGD (http://mips.gsf.de/genre/proj/yeast/). Further details on this quantitative proteomic analysis are given below.

3.2 Mancozeb leads to increased abundance of antioxidant enzymes, chaperone proteins, proteins involved in protein degradation and to the decrease of proteins in protein translation

S. cerevisiae BY4741 adaptation to 2 mg/L of MZ involves the increased content of proteins of the stress response, in particular, antioxidant enzymes. Specifically, the content of the major oxidant scavenging enzymes Cu/Zn and Mn superoxide dismutases (Sod1p and Sod2p), thioredoxin peroxidases Tsa1p and Tsa2p, glutathione peroxidase (Grx1p), NADPH-dependent methylglyoxal reductase (Gre2p), alkyl

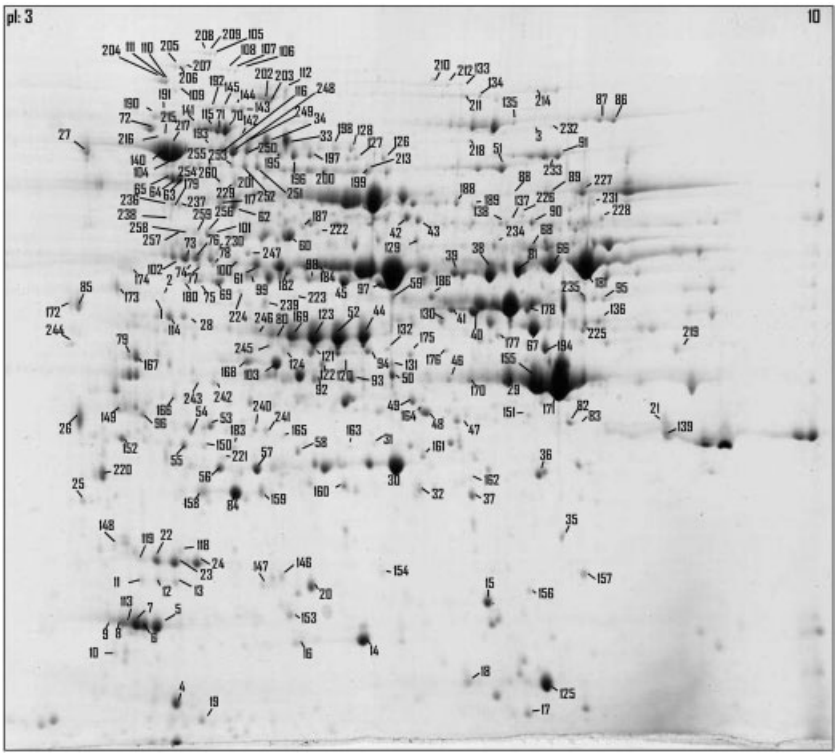

Figure 2. 2-D PAGE-based protein map generated from *S. cerevisiae* BY4741 cells incubated for 5 h with MZ (2 mg/L). IEF was performed between pH 3 and pH 10. Identified spots are indicated and the association with the respective protein name is given in Table A of Supporting Information. This gel is representative of all the gels obtained under this experimental condition.

hydroperoxide reductase (Ahp1p) and thioredoxin-disulphide reductase (Trr1p), increased more than 1.5-fold in response to MZ (Table 1). The antioxidant response registered is consistent with the reported pro-oxidant effect of MZ [8, 9].

Our results also highlighted the importance of several molecular chaperones encoded by heat shock genes in yeast adaptation to MZ. These proteins play an essential role in the cell by assisting the correct folding of nascent and stress-accumulated misfolded proteins and by preventing their aggregation [20]. The proteins whose content increased, under MZ stress, include the *HSP70* family (Ssa1p, Ssa2p, Ssb1p, Ssb2p and Ssc1p), the cochaperones of the *HSP90* family (Sti1p and Sse1p), and Hsp31p, Hsp26p and Hsp104p. The small heat shock protein (sHsp) Hsp26p, after binding misfolded proteins, is known to co-aggregate with them, keeping the entire aggregate in a state that allows efficient disaggregation by the chaperone Hsp104 [20], whose abundance also increases in response to the fungicide.

Remarkably, Hsp104p has been successfully employed to reduce both aggregate formation and cell death in mammalian cell models of Huntington's disease (HD) [21], a devastating neurodegenerative condition associated with the formation of intraneuronal aggregates by mutant huntigtin. Although Hsp104p has no close mammalian ortholog, Hsp104p reduces aggregate formation and prolonged the lifespan of the HD mice [22]. In yeast, Hsp104p facilitates disaggregation and reactivates aggregated proteins with assistance from Ssa1p and Hsp40 (Ydj1p). The content of seven forms of Ssa1p significantly increased (1.5–5.8-fold) under MZ stress, but Hsp40p was not mapped in this study. The reactivation of vital proteins from aggregates is one way to antagonize the detrimental consequences of protein misfolding whenever cellular protein folding is challenged by environmental stress leading to aberrant protein conformation and aggregation. The recovery of proteins from aggregates in the cell therefore requires the chaperones to work together with defined but overlapping function involving several inter-related defence lines against protein aggregation [23]. Hsp26p is an important component of the disaggregation network in *S. cerevisiae* and, in cooperation with the MZ-responsive Hsp104p and the Hsp70 proteins, is thought to promote the efficient clearance of aggregated proteins from the yeast cytosol after stress [20, 23].

Remarkably, the expression of Hsp31p, a member of the DJ-1/ThiJ/Pfp1 superfamily is markedly increased (over 5.5-fold) in response to MZ. Hsp31p expression is also activated in response to heat shock, production of misfolded proteins, oxidative stress by hydrogen peroxide or by the glutathione depletion agent diamide, or by entry into stationary phase caused by carbon starvation [24]. In yeast, Hsp31p protects the cells against oxidative stress, complementing other stress protection systems [25]. Homologues to Hsp31p can be found in eukaryotic and prokaryotic organisms. Interestingly, the human protein DJ-1 when mutated causes hereditary early onset PD [26]. The pathogenesis of this disease is associated with enhanced oxidative stress [27] and protein

Table 1. The relative alteration (above 1.5-fold or below 0.7-fold) of protein content in *S. cerevisiae* BY4741 cells in response to 2 mg/L of MZ

Spot (no.)	Protein description		Fold change (MZ/control)[a)]	ANOVA (p)[b)]
Antioxidants				
8	Ahp1p	Alkyl hydroperoxide reductase	3.7	0.0421
9	Ahp1p		3.3	0.0091
113	Ahp1p		3.0	0.0029
94	Gre2p	NADPH-dependent methylglyoxal reductase	3.8	0.0073
120	Gre2p		4.5	0.0006
122	Gre2p		6.3	0.0020
124	Gre2p		1.5	0.0104
19	Grx1p	GSH peroxidase	1.5	0.0231
16	Sod1p	Cytoplasmatic Cu, Zn SOD	1.6	0.0501
37	Sod2p	Mitochondrial Mn SOD	1.6	0.0045
92	Trr1p	Thioredoxin-disulphide reductase	1.5	0.0077
12	Tsa1p	Thioredoxin peroxidase	4.6	0.0007
13	Tsa1p		3.6	0.0020
154	Tsa2p	Thioredoxin peroxidase	2.7	0.0602
157	Tsa2p		1.6	0.0227
Hsp and chaperones				
202	Hsp104p	Chaperone	2.2	0.0201
203	Hsp104p		2.7	0.0188
155	Hsp26p	sHsp with chaperone activity	5.5	0.0297
56	Hsp31p	Possible chaperone with cysteine-type peptidase; member of the DJ-1/ThiJ/Pfpl superfamily, which includes human DJ-1 involved in PD	6.1	0.0208
57	Hsp31p		5.6	0.0256
64	Hsp60p	Mitochondrial chaperonin	1.5	0.0245
72	Kar2p	Chaperone of the HSP70 family	1.5	0.0612
69	Ssa1p	HSP70 chaperone	5.8	0.0004
75	Ssa1p		4.1	0.0115
104	Ssa1p		1.6	0.0473
215	Ssa1p		1.5	0.0112
217	Ssa1p		2.5	0.0219
224	Ssa1p		2.7	0.0460
239	Ssa1p		2.3	0.0120
10	Ssa2p	HSP70 chaperone	2.4	0.0059
149	Ssa2p		2.1	0.0085
216	Ssa2p		1.8	0.0192
73	Ssb1p	Ribosome-associated molecular chaperone of the HSP70 family	1.6	0.0352
102	Ssb1p		1.5	0.0034
251	Ssb2p	Ribosome-associated molecular chaperone of the HSP70 family	0.7	0.0478
116	Ssc1p	Mitochondrial matrix ATPase of HSP70 family	1.8	0.0153
193	Ssc1p		2.8	0.0898
71	Sse1p	Hsp90 cochaperone	1.9	0.0372
195	Sti1p	Hsp90 cochaperone	1.9	0.0335
196	Sti1p		1.5	0.0138
197	Sti1p		1.9	0.0526
Protein degradation				
146	Pre3p	20S proteasome β-type subunit with endopeptidase activity	1.5	0.0389
82	Pre6p	20S proteasome β-type subunit with endopeptidase activity	1.5	0.0482
58	Pre8p	20S proteasome β-type subunit with endopeptidase activity	1.9	0.0481
54	Pre9p	20S proteasome β-type subunit with endopeptidase activity	1.5	0.0378
Carbohydrate and energetic metabolism				
Glycolysis				
227	Cdc19p	Pyruvate kinase	0.7	0.0032
52	Fba1p	Fructose 1,6-bisphosphate aldolase	0.6	0.0017

Table 1. Continued

Spot (no.)	Protein description		Fold change (MZ/control)[a)]	ANOVA (p)[b)]
21	Gpm1p	Phosphoglycerate mutase	2.5	0.0016
133	Pfk1p	α Subunit of heterooctameric phosphofructokinase	0.6	0.0172
212	Pfk1p		0.7	0.0016
81	Pgk1p	3-Phosphoglycerate kinase	1.5	0.0440
170	Tdh3p	Glyceraldehyde-3-phosphate dehydrogenase	1.7	0.0175
Pyruvate metabolism				
95	Adh3p	Mitochondrial alcohol dehydrogenase isozyme III	0.6	0.0245
42	Ald4p	Mitochondrial aldehyde dehydrogenase	1.8	0.0048
Other				
86	Aco1p	Aconitase	0.5	0.0020
87	Aco1p		0.6	0.0021
176	Qcr2p	Subunit 2 of the ubiquinol–cytochrome *c* reductase complex	1.5	0.0492
55	Sec53p	Phosphomannomutase	0.5	0.0280
150	Sec53p		0.4	0.0157
91	Tkl1p	Transketolase	0.6	0.0035
43	Zwf1p	Glucose-6-phosphate dehydrogenase	1.6	0.0376
Amino acid metabolism				
100	Arg1p	Arginosuccinate synthetase	1.9	0.0616
107	Cpa2p	Large subunit of carbamoyl phosphate synthetase	0.7	0.0043
40	Cys3p	Cystathionine γ-lyase	1.6	0.0504
41	Cys3p		1.8	0.0647
185	Cys3p		2.2	0.0200
90	Cys4p	Cystathionine β-synthase	0.5	0.0059
137	Cys4p		0.6	0.0010
25	Gcv3p	H subunit of the mitochondrial glycine decarboxylase complex	2.3	0.0944
144	His4p	Multifunctional enzyme with phosphoribosyl-ATP pyrophosphatase, phosphoribosyl-AMP cyclohydrolase, and histidinol dehydrogenase activities	0.6	0.0373
145	His4p		0.6	0.0217
192	His4p		0.7	0.0394
231	Ilv3p	Dihydroxyacid dehydratase, involved in the biosynthesis of branched-chain amino acids	0.4	0.0204
3	Lys4p	Homoaconitase	0.4	0.0080
232	Lys4p		0.4	0.0001
135	Met6p	Cobalamin-independent methionine synthase	0.5	0.0033
257	Sam1p	Sam1p	1.5	0.0768
218	Trp5p	Tryptophan synthase	0.5	0.0186
Protein translation				
134	Eft1p	Elongation factor 2	0.7	0.0033
162	Rps5p	Protein component of the small (40S) Ribosomal subunit	0.4	0.0471
119	Tif11p	Translation initiation factor eIF1A	0.6	0.0431
Vacuolar function				
85	Pep4p	Vacuolar aspartyl protease (proteinase A)	2.0	0.0004
48	Prb1p	Vacuolar proteinase B	2.0	0.0360
255	Vma1p	Vacuolar H+-ATPase V1 domain subunit	0.6	0.0472
237	Vma2p	Subunit B of the eight-subunit V1 peripheral membrane domain of the vacuolar H+-ATPase	0.5	0.0134
183	Vma4p	Subunit E of the eight-subunit V1 peripheral membrane domain of the vacuolar H+-ATPase	0.3	0.0039
Other functions				
214	Ade3p	Cytoplasmic trifunctional enzyme C1-tetrahydrofolate synthase, involved in single carbon metabolism and required for biosynthesis of purines, thymidylate, methionine, and histidine	1.8	0.0473

Table 1. Continued

Spot (no.)	Protein description		Fold change (MZ/control)[a)]	ANOVA (p)[b)]
2	Apa1p	Bis(5′-nucleosyl)-tetraphosphatase	0.3	0.0266
244	Clc1p	Clathrin light chain	0.6	0.0005
35	Frm2p	Putative NADPH-dependent FMN-containing oxidoreductase	4.3	0.0106
15	Hbn1p	Putative NADPH-dependent FMN-containing oxidoreductase	6.4	0.0775
38	Oye2p	Widely conserved NADPH oxidoreductase-containing FMN	1.7	0.0013
39	Oye2p		2.5	0.0593
182	Oye3p	Widely conserved NADPH oxidoreductase-containing FMN	2.8	0.0018
126	Pab1p	Poly(A) binding protein	0.3	0.0082
127	Pab1p		0.6	0.0040
130	Psa1p	GDP-mannose pyrophosphorylase	0.6	0.0313
20	Pst2p	Biological process unknown	3.2	0.0452
ORF's				
50	Ydl124wp	NADPH-dependent α-keto amide reductase	2.6	0.0006
131	Ydl124wp		2.1	0.0646
235	Ylr460cp	Biological process unknown	2.3	0.0142
160	Ymr090wp	Biological process unknown	1.6	0.0064
45	Ynl134cp	Alcohol dehydrogenase (NADP+) activity	2.4	0.0214
97	Ynl134cp		2.5	0.0037
98	Ynl134cp		2.0	0.0009

Ratio values (fold change) of normalized protein spots intensities, in 2-DE gels, obtained from cells of *S. cerevisiae* BY4741 grown in MZ-supplemented medium *versus* cells grown in basal medium. The strongest alterations (above 2.0-fold or below 0.5-fold) are shaded in grey.

a) Values were calculated as the average data from, at least, three independent experiments and data were filtered to retain spots with ANOVA *p.*

b) Values of 0.05 or less to ensure high statistical confidence of differential expression. In some specific cases results with ANOVA *p* values (underlined) up to 0.1 are shown.

aggregation, and fibrillation [28]. The oxidative stress activated chaperone DJ-1, also acting as a free radical scavenger, contributes to the protection against enhanced oxidative stress in PD [26–29].

Proteins involved in protein degradation, in particular, the 20S proteasome subunits Pre3p, Pre6p, Pre8p and Pre9p, also exhibited increased levels in response to MZ (Table 1). The yeast 20S proteasome is a soluble complex with proteolytic activity and a component of the ATP-dependent 26S proteasome holoenzyme, a highly conserved structure among eukaryotes involved in the degradation of ubiquitin-conjugated proteins [30]. According to evidences, the yeast 20S proteasome can also degrade oxidatively modified proteins even in the absence of ATP and ubiquitination [31, 32]. The upregulation of the 20S proteasome was also registered in response to oxidative stress by yeast exposure to H_2O_2 [31, 32], which suggests that this MZ response may reflect the enhanced accumulation of oxidized proteins. The MZ-induced increase in the amount of the vacuolar proteases Prb1p and Pep4p, involved in the degradation of the cargo delivered to the vacuole by autophagy or other secretory pathways [33], was also registered. The involvement of Pep4p in post-translational precursor maturation of vacuolar proteases was also proposed [33]. Taken together, these results are consistent with the induction of a cellular response for the rapid elimination of misfolded proteins presumably present in MZ-stressed cells, thus promoting the necessary alteration of the internal protein repertoire [34].

A general decrease in the amount of a number of proteins involved in protein translation was registered during adaptation to MZ stress; Tif11p, a translation initiation factor [35], Eft1p a translation elongation factor [36], and one form of Rps5p, a component of the small (40S) ribosomal subunit [37]. This cell response suggests that MZ induce a decrease in protein synthesis which is a feature of the environment stress response programme in yeast [34], consistent with the need to focus cell machinery in response to stress prior to growth resumption and the maintenance of protein translation fidelity at the expense of global protein synthesis rate.

3.3 Mancozeb leads to alterations in the content of proteins of carbohydrate, energy and aminoacid metabolism

The alteration of the level of 13 MZ-responsive proteins involved in carbohydrate and energy metabolism in response to MZ suggest a MZ-induced redistribution of the

metabolic fluxes, characterized by a shift in the balance between glycolysis and the pentose phosphate pathway. In MZ-stressed cells, the content of Pfk1p is reduced. Pfk1p is one of the two subunits that compose the hetero-octamer 6-phosphofructo-1-kinase that catalyses an irreversible reaction in the glycolytic pathway. MZ also induced the increased abundance of glucose-6-phosphate dehydrogenase (Zwf1p). Zwf1p regulates the carbon flow through the pentose phosphate pathway by catalyzing its first oxidative step and is required for yeast adaptation to oxidative stress [38]. The hypothesized shift of glucose metabolism from glycolysis to the pentose phosphate pathway, presumably leads to the generation of NADPH which provides the reducing power for antioxidant enzymes. The increased abundance in response to MZ of Oye2p, Oye3p, two putative NADPH oxidoreductases, containing flavin mononucleotide (FMN) as prosthetic group and proposed to be involved in sterol metabolism [39] and Ynl134cp (a NADPH-dependent alcohol dehydrogenase) suggest that this response may also be involved in the maintenance of NADPH redox balance, as hypothesized for yeast response to arsenite [40]. Expression of Ynl134cp was first identified as being activated in response to stress induced by the DNA-damaging agent methyl methanesulphonate (MMS) [41]. Frm2p and Hbn1p, whose abundance also increased in response to MZ, are additional putative FMN-containing NADPH oxidoreductases [42]. Frm2p was implicated in lipid signalling pathway and cellular homeostasis [43] and single or double mutants for *FRM2* and *HBN1* genes are extremely sensitive to nitrosative stress inducing substances such as 4-nitroquinoline 1-oxide (4-NQO) [42]. Pst2p, whose abundance was also increased following cell exposure to MZ, is a protein with similarity to members of a family of flavodoxin-like proteins that is upregulated in response to oxidative stress [44].

In MZ-stressed yeast cells there is a decrease in the amount of a large number of enzymes involved in amino acid biosynthesis (Table 1), as observed before under hydrogen peroxide stress [45]. The relevant exceptions are the enzymes components of the sulphur assimilation and glutathione biosynthetic pathways. The content of cystathionine γ-lyase (Cys3p), the last enzyme of cysteine biosynthetic pathway, and *S*-adenosylmethionine synthetase (Sam1p), required for the methyl cycle pathway and for the synthesis of the molecular weight thiol molecule *S*-adenosylmethionine, were found in higher abundance in MZ exposed cells. Although the rate limiting enzyme of glutathione biosynthesis, Gsh1p, was not mapped in this study, the increased level of Cys3p and the fact that the mutant with the corresponding gene deleted is strongly sensitive to MZ (Dias and Sá-Correia, unpublished results), suggests that the flux of sulphur could be redirected towards *S*-adenosylmethionine and glutathione (GSH) as proposed for the yeast cell response to cadmium [46]. The tripeptide GSH is an important molecule in cell protection against oxidative stress and metal toxicity. Indeed, cysteine SH groups are among the most easily oxidized residues and oxidative stress can cause intracellular protein crosslinking and enzyme inactivation. Such irreversible oxidation can be prevented by protein S-thiolation in which protein SH groups form mixed disulphides with other low molecular weight thiols such as GSH. MZ biological effects are considered to involve a mechanism based on modification of key reactive thiols [12], as suggested for the mechanism through which celastrol carries out its effects in yeast [47].

Although, vacuolar H^+-ATPase plays an important physiological role following yeast exposure to severe oxidative stress situations [48], a decrease of the content of the vacuolar H^+-ATPase subunits Vma1p, Vma2p and Vma4p, was registered under MZ stress. This response may reduce ATP consumption under less favourable energetic conditions [49], thus allowing ATP to be spared for other energy-dependent adaptation mechanisms under MZ stress.

3.4 The complex coordinate regulation of the yeast response to mancozeb

More than 90% of genes encoding proteins whose content increased in response to MZ are known targets of the transcription factor Yap1p (Table 2 and Table C of Supporting Information), according to the information gathered in YEASTRACT [50, 51]. This information system was used in this study to predict the transcription factors underlying the coordinate transcription activation of the over-expressed genes under MZ stress (Table C of Supporting Information). Yap1p is a determinant of yeast resistance to MZ [15] and one of the main regulators of the oxidative stress response in yeast [44]. The very important role suggested for Yap1p in yeast adaptive response to MZ is also consistent with the hypothesized pro-oxidant action of this fungicide and the potential involvement of Met4p and Skn7p, in coordination with Yap1p, in the upregulation of 50 and 27% of the genes encoding the MZ responsive proteins identified, respectively. The leucine zipper transcription activator Met4p is responsible for the regulation of the sulphur aminoacid pathway and oxidative stress response genes and Skn7p is required for optimal induction of heat shock genes in response to oxidative stress. This study also pinpointed a number of other transcription factors that might control the response to MZ, including Msn2p and Msn4p, the main regulators of the environmental stress response (ESR) program, that regulate, directly or indirectly, 46–50% of the genes encoding proteins whose abundance increased in response to MZ, and Pdr1p, the master regulator to fine tune the regulation of multidrug resistance genes [52], which regulates 27% of the same dataset. They also include Rpn4p which controls the expression of 26S proteasome genes, consistent with MZ-induced

Table 2. MZ responsive genes grouped by transcription factor (TF) involved in their regulation

Transcription factor	%	ORF/genes
Yap1p	91.1	SSA1, CYS3, HSP26, FRM2, HBN1, GRX1, PGK1, YDL124w, PST2, TRR1, TSA2, HSP31, PRB1, PRE9, TDH3, ADE3, SOD2, OYE2, KAR2, SSC1, SOD1, SSA2, HSP104, AHP1, SAM1, HSP60, YLR460c, TSA1, PRE8, YMR090w, YNL134c, ZWF1, PRE6, ARG1, GRE2, STI1, ALD4, SSE1, PEP4, OYE3, QCR2
Msn2p	48.9	SSA1, HSP26, GRX1, YDL124w, PST2, TRR1, TSA2, HSP31, TDH3, SOD2, SSC1, GPM1, SSA2, HSP104, AHP1, TSA1, YMR090w, YNL134c, GRE2, ALD4, PEP4, OYE3
Msn4p	46.7	SSA1, HSP26, GRX1, YDL124w, PST2, TRR1, TSA2, HSP31, TDH3, SOD2, SSA2, HSP104, AHP1, TSA1, YMR090w, YNL134c, ZWF1, GRE2, ALD4, PEP4, OYE3
Met4p	42.2	CYS3, GCV3, HSP26, PGK1, HSP31, PRB1, ADE3, SOD2, SSC1, SOD1, HSP104, SAM1, PRE8, YMR090w, PRE6, ARG1, STI1, ALD4, OYE3
Hsf1p	42.2	SSA1, HSP26, PGK1, TDH3, SOD2, OYE2, KAR2, SSC1, GPM1, SSA2, HSP104, AHP1, HSP60, YNL134c, PRE6, GRE2, STI1, ALD4, SSE1
Aft1p	40.0	SSA1, HSP26, YDL124w, TSA2, HSP31, PRB1, SOD2, PRE3, SOD1, SSA2, HSP104, AHP1, HSP60, ZWF1, STI1, ALD4, PEP4, OYE3
Pdr1p	26.7	HSP26, TRR1, HSP31, TDH3, SSA2, HSP104, AHP1, SAM1, YNL134c, ZWF1, GRE2, ALD4
Skn7p	26.7	SSA1, HSP26, TRR1, TSA2, SOD2, SOD1, HSP104, AHP1, TSA1, ARG1, GRE2, OYE3
Rpn4p	24.4	GCV3, FRM2, HBN1, PGK1, TRR1, PRE9, PRE3, YLR460c, PRE8, PRE6, ARG1
Gcn4p	17.8	CYS3, GCV3, HSP26, FRM2, TDH3, ADE3, SOD1, ARG1

TF are ordered by the decreased percentage of regulated genes, relative to the total number of genes encoding proteins whose abundance increased following MZ stress in *S. cerevisiae*. This gene clustering was based on the information and tools available in YEASTRACT database [51] in May 2008. The full list of TF is presented in Table C of the Supporting Information.

protein inactivation and consequent protein degradation *via* the proteasome. By eliminating improperly folded damaged protein, the ubiquitin/proteasome proteolytic pathway is of vital importance in the defence against cellular damage caused by xenobiotic compounds. It is also conceivable that the proteasome activity is sensitive to MZ-induced damage, as reported for neuronal cell lines [53], leading to dysfunctional protein turnover that may be partially compensated by the increased availability of 26S proteasome subunits. Gcn4p is also a possible regulator of about 20% of the genes encoding MZ-induced proteins. This transcriptional regulator of aminoacid biosynthetic genes in response to aminoacid starvation [54], eventually resulting from the disruption of aminoacid uptake by MZ, also plays an essential and previously unrecognized role in the unfolded protein response (UPR) by modulating it [55], consistent with the hypothesized protein denaturating effects associated to MZ stress. Another transcription factor known to control the activation of 40% of the upregulated genes in response to MZ is Aft1p, which activates the expression of target genes in response to changes in iron availability. Interestingly, high zinc levels leads to decreased intracellular iron content [56]. Although MZ supplementation may result in an increase of the zinc concentration in the growth medium, it is questionable if the levels attained are enough to induce this cell response.

MZ also induced the heat shock response (HSR), a highly conserved cytoprotective mechanism. Increased production of Hsp, in particular protein chaperones is essential for the folding stability, trafficking, repair and degradation of damaged proteins, thus, promoting protection against acute cell injury. The HSR is regulated by the stress-inducible heat shock transcription factor Hsf1p, conserved from yeast to man. *S. cerevisiae* Hsf1p is predicted to regulate 42% of the genes encoding the proteins whose content increased under MZ stress. It is known that Hsf1p was found to activate the transcription of various target genes when yeast cells are treated with oxidizing agents, including superoxide generators and thiol oxidants [57], acting with Msn2p/Msn4p, Skn7p and Yap1p, to efficiently activate the transcription of the respective target genes under oxidative stress.

More than 20% of the group of MZ downregulated genes are predicted to be regulated by Sfp1p, a transcription factor that is released from the promoters of ribosomal protein genes under stress leading to decreased expression of ribosome biogenesis genes in response to stress. The target genes include the three proteins (Eft1p, Rps5p and Tif11p) involved in protein translation whose content decreases under MZ stress.

3.5 Adaptive response to mancozeb: Human orthologs and protein–protein interactions

The yeast adaptive responses to MZ deleterious effects emerging from this proteomic analysis may be extended to the phytopathogenic fungi that are the natural targets of this agricultural fungicide. This global response may also provide clues to understand MZ toxicity in humans as 70% of the proteins identified as having an altered expression level in response to MZ have human orthologs (Table D of Supporting Information), while the whole yeast genome only includes about 30% proteins with human homologues. For example, HSPA5, the human ortholog of the yeast chaperone Kar2p, is associated with ER stress response which plays a critical role in the regulation of protein synthesis, protein folding and trafficking. Activation of the ER stress response is known to lead to attenuation of protein synthesis, the translocation of unfolded or misfolded proteins and their degradation by the ubiquitin/proteasome system, induction of chaperone synthesis to increase folding capacity and induction of apoptosis [58]. Superoxide dismutase 1 and 2 (SOD1 and SOD2) are the human orthologs of yeast Sod1p and Sod2p, respectively. Recent evidence suggests that SOD1 may play a role in the onset and progression of PD and its induction may act neuroprotectively [59]. The heat shock 70 kDa protein 9, HSPA9, the human ortholog of the yeast heat shock 70 kDa protein Ssc1p, was implicated in multiple functions ranging from stress response, intracellular trafficking, antigen processing, control of cell proliferation, differentiation and tumorigenesis [60] and the human ortholog of Sse1p, the heat shock 70 kDa protein 4, HSPA4, is a key molecule in induction of adaptive response to radiation [61] and thought to play an important role in the maintenance of neuronal functions under physiological and stress conditions [62]. The human ortholog of yeast Tsa1p is the peroxiredoxin 2 PRDX2. Peroxiredoxins are a ubiquitously expressed family of thiol peroxidases. Oxidative stress elicited by amyloid β (Aβ) accumulation is a causative factor in the pathogenesis of Alzheimer disease (AD) and Abeta-resistant PC12 cell lines exhibit increased expression of multiple Prx isoforms with reduced cysteine oxidation [63]. Additionally, depletion of the human ortholog of yeast Tsa2p, the peroxiredoxin 3, PRDX3, resulted in increased intracellular levels of H_2O_2 and sensitized cells to induction of apoptosis, suggesting that PRDX3 is a critical regulator of the abundance of mitochondrial H_2O_2, which itself promotes apoptosis in cooperation with other mediators of apoptotic signaling [64].

PSMA2, PSMA4, PSMA7 and PSMB6, are different proteasome subunits and the human orthologs of yeast Pre8p, Pre9p, Pre7p and Pre3p, respectively. A functional ubiquitin/proteasome system is essential for all eukaryotic cells and any alteration to its components has potential pathological consequences. Although the exact underlying mechanism is still unclear, an age-related decrease in proteasome activity weakens cellular capacity to remove oxidatively modified proteins and favours the development of neurodegenerative and cardiac diseases [65]. In human cell lines, overexpression of proteasome subunits increased rate of survival following oxidative stress, due to higher proteasome degradation rates [66].

Protein–protein associations in the dataset of yeast proteins whose abundance changed in response to MZ were predicted using the database STRING [67]. Having in mind that studies on yeast orthologs to human proteins have already generated significant insights into human diseases [68], the same exercise was carried out for human orthologs to the referred yeast proteins (Table D of Supporting Information). The result of this analysis is shown in Fig. 3 and the analogy of the main interaction groups in the two biological systems reinforce the idea that the indications obtained from this study may be useful to get insights into the global response to MZ toxicity in humans.

4 Concluding remarks

The toxicoproteomics analysis carried out in this study allowed the monitoring of the early steps of the adaptive response to a growth inhibitory concentration of the fungicide MZ in yeast, focusing on the subproteome of the soluble proteins with a p*I* between 3 and 10. The main functional groups of proteins whose abundance was affected by MZ challenge include proteins associated with the antioxidant response, carbohydrate and energy metabolism, protein chaperone activity, protein synthesis and protein degradation through the proteasome. The generated networks of protein–protein associations of yeast proteins whose abundance changed in response to MZ and of their human orthologs share a high degree of similarity. This observation suggests that the main conclusions of this study can be considered as powerful indications to expand the knowledge obtained in yeast not only to the global response to MZ toxicity in phytopathogenic fungi but also to humans.

This research was supported by FEDER and "Fundação para a Ciência e Tecnologia" (FCT) (contract PTDC/BIO/72063/2006).

The authors have declared no conflict of interest.

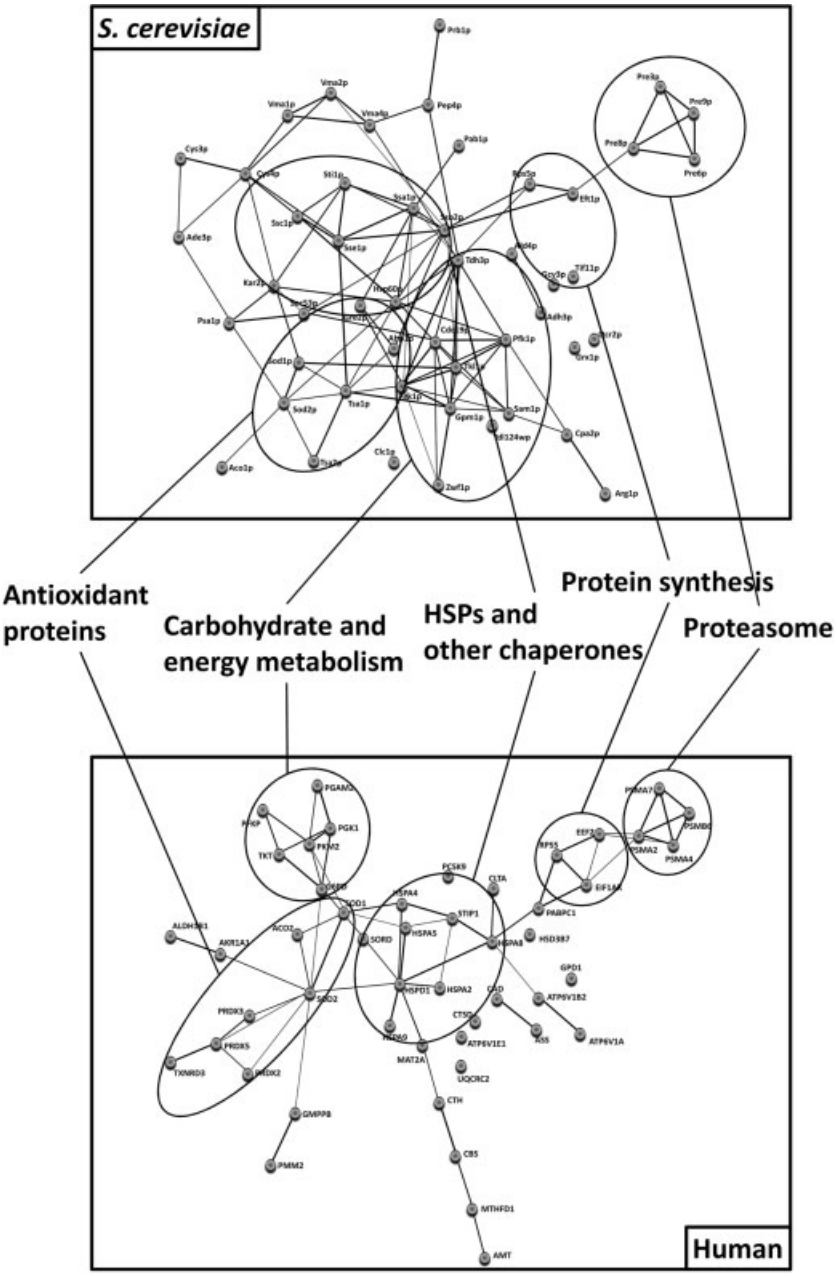

Figure 3. Graphical representations of protein interaction networks in *S. cerevisiae* and in *Homo sapiens*, adapted from the output of STRING database [67], using the default parameters. The proteins used in this comparison were the MZ responsive yeast proteins with human orthologs. The full list of human orthologs is shown in Table D of Supporting Information. Stronger associations are represented with thicker connecting lines whereas weaker associations are represented by thinner connecting lines.

5 References

[1] Cory-Slechta, D. A., Thiruchelvam, M., Barlow, B. K., Richfield, E. K., Developmental pesticide models of the Parkinson disease phenotype. *Environ. Health Perspect.* 2005, *113*, 1263–1270.

[2] Gerber, G. B., Leonard, A., Hantson, P., Carcinogenicity, mutagenicity and teratogenicity of manganese compounds. *Crit. Rev. Oncol. Hematol.* 2002, *42*, 25–34.

[3] Meco, G., Bonifati, V., Vanacore, N., Fabrizio, E., Parkinsonism after chronic exposure to the fungicide maneb (manganese ethylene-bis-dithiocarbamate). *Scand. J. Work Environ. Health* 1994, *20*, 301–305.

[4] Thiruchelvam, M., McCormack, A., Richfield, E. K., Baggs, R. B. *et al.*, Age-related irreversible progressive nigrostriatal dopaminergic neurotoxicity in the paraquat and maneb model of the Parkinson's disease phenotype. *Eur. J. Neurosci.* 2003, *18*, 589–600.

[5] Kamel, F., Engel, L. S., Gladen, B. C., Hoppin, J. A. *et al.*, Neurologic symptoms in licensed private pesticide applicators in the agricultural health study. *Environ. Health Perspect.* 2005, *113*, 877–882.

[6] Baligar, P. N., Kaliwal, B. B., Induction of gonadal toxicity to female rats after chronic exposure to mancozeb. *Ind. Health* 2001, *39*, 235–243.

[7] Kackar, R., Srivastava, M. K., Raizada, R. B., Studies on rat thyroid after oral administration of mancozeb: Morphological and biochemical evaluations. *J. Appl. Toxicol.* 1997, *17*, 369–375.

[8] Domico, L. M., Cooper, K. R., Bernard, L. P., Zeevalk, G. D., Reactive oxygen species generation by the ethylene-bisdithiocarbamate (EBDC) fungicide mancozeb and its contribution to neuronal toxicity in mesencephalic cells. *Neurotoxicology* 2007, *28*, 1079–1091.

[9] Calviello, G., Piccioni, E., Boninsegna, A., Tedesco, B. *et al.*, DNA damage and apoptosis induction by the pesticide Mancozeb in rat cells: Involvement of the oxidative mechanism. *Toxicol. Appl. Pharmacol.* 2006, *211*, 87–96.

[10] Maroni, M., Colosio, C., Ferioli, A., Fait, A., Biological Monitoring of Pesticide Exposure: A review. Introduction. *Toxicology* 2000, *143*, 1–118.

[11] Allain, P., Krari, N., Diethyldithiocarbamate, copper and neurological disorders. *Life Sci.* 1991, *48*, 291–299.

[12] Vaccari, A., Saba, P., Mocci, I., Ruiu, S., Dithiocarbamate pesticides affect glutamate transport in brain synaptic vesicles. *J. Pharmacol. Exp. Ther.* 1999, *288*, 1–5.

[13] Teixeira, M. C., Duque, P., Sa-Correia, I., Environmental genomics: Mechanistic insights into toxicity of and resistance to the herbicide 2,*4*-D. *Trends Biotechnol.* 2007, *25*, 363–370.

[14] Simmons, P. T., Portier, C. J., Toxicogenomics: The new frontier in risk analysis. *Carcinogenesis* 2002, *23*, 903–905.

[15] Teixeira, M. C., Dias, P. J., Simoes, T., Sa-Correia, I., Yeast adaptation to mancozeb involves the upregulation of FLR1 under the coordinate control of Yap1, Rpn4, Pdr3, and Yrr1. *Biochem. Biophys. Res. Commun.* 2008, *367*, 249–255.

[16] Santos, P. M., Benndorf, D., Sa-Correia, I., Insights into *Pseudomonas putida* KT2440 response to phenol-induced stress by quantitative proteomics. *Proteomics* 2004, *4*, 2640–2652.

[17] Shevchenko, A., Tomas, H., Havlis, J., Olsen, J. V., Mann, M., In-gel digestion for mass spectrometric characterization of proteins and proteomes. *Nat. Protoc.* 2006, *1*, 2856–2860.

[18] Suckau, D., Resemann, A., Schuerenberg, M., Hufnagel, P. *et al.*, A novel MALDI LIFT-TOF/TOF mass spectrometer for proteomics. *Anal. Bioanal. Chem.* 2003, *376*, 952–965.

[19] Perkins, D. N., Pappin, D. J., Creasy, D. M., Cottrell, J. S., Probability-based protein identification by searching sequence databases using mass spectrometry data. *Electrophoresis* 1999, *20*, 3551–3567.

[20] Cashikar, A. G., Duennwald, M., Lindquist, S. L., A chaperone pathway in protein disaggregation. Hsp26 alters the nature of protein aggregates to facilitate reactivation by Hsp104. *J. Biol. Chem.* 2005, *280*, 23869–23875.

[21] Carmichael, J., Chatellier, J., Woolfson, A., Milstein, C. *et al.*, Bacterial and yeast chaperones reduce both aggregate formation and cell death in mammalian cell models of Huntington's disease. *Proc. Natl. Acad. Sci. USA* 2000, *97*, 9701–9705.

[22] Vacher, C., Garcia-Oroz, L., Rubinsztein, D. C., Overexpression of yeast hsp104 reduces polyglutamine aggregation and prolongs survival of a transgenic mouse model of Huntington's disease. *Hum. Mol. Genet.* 2005, *14*, 3425–3433.

[23] Haslbeck, M., Miess, A., Stromer, T., Walter, S., Buchner, J., Disassembling protein aggregates in the yeast cytosol. The cooperation of Hsp26 with Ssa1 and Hsp104. *J. Biol. Chem.* 2005, *280*, 23861–23868.

[24] Wilson, M. A., St Amour, C. V., Collins, J. L., Ringe, D., Petsko, G. A., The 1.8-A resolution crystal structure of YDR533Cp from *Saccharomyces cerevisiae*: A member of the DJ-1/ThiJ/Pfpl superfamily. *Proc. Natl. Acad. Sci. USA* 2004, *101*, 1531–1536.

[25] Skoneczna, A., Micialkiewicz, A., Skoneczny, M., *Saccharomyces cerevisiae* Hsp31p, a stress response protein conferring protection against reactive oxygen species. *Free Radic. Biol. Med.* 2007, *42*, 1409–1420.

[26] Moore, D. J., Zhang, L., Troncoso, J., Lee, M. K. *et al.*, Association of DJ-1 and parkin mediated by pathogenic DJ-1 mutations and oxidative stress. *Hum. Mol. Genet.* 2005, *14*, 71–84.

[27] Zhang, L., Shimoji, M., Thomas, B., Moore, D. J. *et al.*, Mitochondrial localization of the Parkinson's disease related protein DJ-1: Implications for pathogenesis. *Hum. Mol. Genet.* 2005, *14*, 2063–2073.

[28] Zhou, W., Zhu, M., Wilson, M. A., Petsko, G. A., Fink, A. L., The oxidation state of DJ-1 regulates its chaperone activity toward alpha-synuclein. *J. Mol. Biol.* 2006, *356*, 1036–1048.

[29] Dawson, T. M., Dawson, V. L., Molecular pathways of neurodegeneration in Parkinson's disease. *Science* 2003, *302*, 819–822.

[30] Glickman, M. H., Ciechanover, A., The ubiquitin-proteasome proteolytic pathway: Destruction for the sake of construction. *Physiol. Rev.* 2002, *82*, 373–428.

[31] Davies, K. J., Shringarpure, R., Preferential degradation of oxidized proteins by the 20S proteasome may be inhibited in aging and in inflammatory neuromuscular diseases. *Neurology* 2006, *66*, S93–S96.

[32] Khan, M. A., Chock, P. B., Stadtman, E. R., Knockout of caspase-like gene, YCA1, abrogates apoptosis and elevates oxidized proteins in *Saccharomyces cerevisiae*. *Proc. Natl. Acad. Sci. USA* 2005, *102*, 17326–17331.

[33] Van Den Hazel, H. B., Kielland-Brandt, M. C., Winther, J. R., Review: Biosynthesis and function of yeast vacuolar proteases. *Yeast* 1996, *12*, 1–16.

[34] Gasch, A. P., Werner-Washburne, M., The genomics of yeast responses to environmental stress and starvation. *Funct. Integr. Genomics* 2002, *2*, 181–192.

[35] Olsen, D. S., Savner, E. M., Mathew, A., Zhang, F. *et al.*, Domains of eIF1A that mediate binding to eIF2, eIF3 and eIF5B and promote ternary complex recruitment in vivo. *EMBO J.* 2003, *22*, 193–204.

[36] Justice, M. C., Hsu, M. J., Tse, B., Ku, T. *et al.*, Elongation factor 2 as a novel target for selective inhibition of fungal protein synthesis. *J. Biol. Chem.* 1998, *273*, 3148–3151.

[37] Planta, R. J., Mager, W. H., The list of cytoplasmic ribosomal proteins of *Saccharomyces cerevisiae*. *Yeast* 1998, *14*, 471–477.

[38] Izawa, S., Maeda, K., Miki, T., Mano, J. *et al.*, Importance of glucose-6-phosphate dehydrogenase in the adaptive response to hydrogen peroxide in *Saccharomyces cerevisiae*. *Biochem. J.* 1998, *330*, 811–817.

[39] Stott, K., Saito, K., Thiele, D. J., Massey, V., Old Yellow Enzyme. The discovery of multiple isozymes and a family of related proteins. *J. Biol. Chem.* 1993, *268*, 6097–6106.

[40] Thorsen, M., Lagniel, G., Kristiansson, E., Junot, C. *et al.*, Quantitative transcriptome, proteome, and sulfur metabolite profiling of the *Saccharomyces cerevisiae* response to arsenite. *Physiol. Genomics* 2007, *30*, 35–43.

[41] Lee, M. W., Kim, B. J., Choi, H. K., Ryu, M. J. *et al.*, Global protein expression profiling of budding yeast in response to DNA damage. *Yeast* 2007, *24*, 145–154.

[42] de Oliveira, I. M., Henriques, J. A., Bonatto, D., In silico identification of a new group of specific bacterial and fungal nitroreductases-like proteins. *Biochem. Biophys. Res. Commun.* 2007, *355*, 919–925.

[43] McHale, M. W., Kroening, K. D., Bernlohr, D. A., Identification of a class of *Saccharomyces cerevisiae* mutants defective in fatty acid repression of gene transcription and analysis of the frm2 gene. *Yeast* 1996, *12*, 319–331.

[44] Lee, J., Godon, C., Lagniel, G., Spector, D. *et al.*, Yap1 and Skn7 control two specialized oxidative stress response regulons in yeast. *J. Biol. Chem.* 1999, *274*, 16040–16046.

[45] Godon, C., Lagniel, G., Lee, J., Buhler, J. M. *et al.*, The H_2O_2 stimulon in *Saccharomyces cerevisiae*. *J. Biol. Chem.* 1998, *273*, 22480–22489.

[46] Lafaye, A., Junot, C., Pereira, Y., Lagniel, G. *et al.*, Combined proteome and metabolite-profiling analyses reveal surprising insights into yeast sulfur metabolism. *J. Biol. Chem.* 2005, *280*, 24723–24730.

[47] Trott, A., West, J. D., Klaic, L., Westerheide, S. D. Activation of heat shock and antioxidant responses by the natural product celastrol: Transcriptional signatures of a thiol-targeted molecule. *Mol. Biol. Cell.* 2008.

[48] Milgrom, E., Diab, H., Middleton, F., Kane, P. M., Loss of vacuolar proton-translocating ATPase activity in yeast results in chronic oxidative stress. *J. Biol. Chem.* 2007, *282*, 7125–7136.

[49] Kane, P. M., Parra, K. J., Assembly and regulation of the yeast vacuolar H(+)-ATPase. *J. Exp. Biol.* 2000, *203*, 81–87.

[50] Monteiro, P. T., Mendes, N. D., Teixeira, M. C., d'Orey, S. *et al.*, YEASTRACT-DISCOVERER: New tools to improve the analysis of transcriptional regulatory associations in *Saccharomyces cerevisiae*. *Nucleic Acids Res.* 2008, *36*, D132–D136.

[51] Teixeira, M. C., Monteiro, P., Jain, P., Tenreiro, S. *et al.*, The YEASTRACT database: A tool for the analysis of transcription regulatory associations in *Saccharomyces cerevisiae*. *Nucleic Acids Res.* 2006, *34*, D446–D451.

[52] Hallstrom, T. C., Moye-Rowley, W. S., Divergent transcriptional control of multidrug resistance genes in *Saccharomyces cerevisiae*. *J. Biol. Chem.* 1998, *273*, 2098–2104.

[53] Zhou, Y., Shie, F. S., Piccardo, P., Montine, T. J., Zhang, J., Proteasomal inhibition induced by manganese ethylene-bis-dithiocarbamate: Relevance to Parkinson's disease. *Neuroscience* 2004, *128*, 281–291.

[54] Hinnebusch, A. G., Translational regulation of GCN4 and the general amino acid control of yeast. *Annu. Rev. Microbiol.* 2005, *59*, 407–450.

[55] Patil, C. K., Li, H., Walter, P., Gcn4p and novel upstream activating sequences regulate targets of the unfolded protein response. *PLoS Biol.* 2004, *2*, 1208–1223.

[56] Pagani, M. A., Casamayor, A., Serrano, R., Atrian, S., Arino, J., Disruption of iron homeostasis in *Saccharomyces cerevisiae* by high zinc levels: A genome-wide study. *Mol. Microbiol.* 2007, *65*, 521–537.

[57] Yamamoto, A., Ueda, J., Yamamoto, N., Hashikawa, N., Sakurai, H., Role of heat shock transcription factor in *Saccharomyces cerevisiae* oxidative stress response. *Eukaryotic Cell* 2007, *6*, 1373–1379.

[58] Joo, J. H., Liao, G., Collins, J. B., Grissom, S. F., Jetten, A. M., Farnesol-induced apoptosis in human lung carcinoma cells is coupled to the endoplasmic reticulum stress response. *Cancer Res.* 2007, *67*, 7929–7936.

[59] Ihara, Y., Nobukuni, K., Takata, H., Hayabara, T., Oxidative stress and metal content in blood and cerebrospinal fluid of amyotrophic lateral sclerosis patients with and without a Cu, Zn-superoxide dismutase mutation. *Neurol. Res.* 2005, *27*, 105–108.

[60] Wadhwa, R., Taira, K., Kaul, S. C., An Hsp70 family chaperone, mortalin/mthsp70/PBP74/Grp75: What, when, and where? *Cell Stress Chaperones* 2002, *7*, 309–316.

[61] Kang, C. M., Park, K. P., Cho, C. K., Seo, J. S. *et al.*, Hspa4 (HSP70) is involved in the radioadaptive response: Results from mouse splenocytes. *Radiat. Res.* 2002, *157*, 650–655.

[62] Okui, M., Ito, F., Ogita, K., Kuramoto, N. *et al.*, Expression of APG-2 protein, a member of the heat shock protein 110 family, in developing rat brain. *Neurochem. Int.* 2000, *36*, 35–43.

[63] Cumming, R. C., Dargusch, R., Fischer, W. H., Schubert, D., Increase in expression levels and resistance to sulfhydryl oxidation of peroxiredoxin isoforms in amyloid beta-resistant nerve cells. *J. Biol. Chem.* 2007, *282*, 30523–30534.

[64] Chang, T. S., Cho, C. S., Park, S., Yu, S. *et al.*, Peroxiredoxin III, a mitochondrion-specific peroxidase, regulates apoptotic signaling by mitochondria. *J. Biol. Chem.* 2004, *279*, 41975–41984.

[65] Dahlmann, B., Role of proteasomes in disease. *BMC Biochem.* 2007, *8*, S3.

[66] Chondrogianni, N., Tzavelas, C., Pemberton, A. J., Nezis, I. P. *et al.*, Overexpression of proteasome beta5 assembled subunit increases the amount of proteasome and confers ameliorated response to oxidative stress and higher survival rates. *J. Biol. Chem.* 2005, *280*, 11840–11850.

[67] von Mering, C., Jensen, L. J., Kuhn, M., Chaffron, S. *et al.*, STRING 7–recent developments in the integration and prediction of protein interactions. *Nucleic Acids Res.* 2007, *35*, D358–D362.

[68] Hsu, W. T., Pang, C. N., Sheetal, J., Wilkins, M. R., Protein-protein interactions and disease: Use of *S. cerevisiae* as a model system. *Biochim. Biophys. Acta* 2007, *1774*, 838–847.

